U_{ii} <0·05], 19 (29%) were discarded by the same accuracy test. This result indicates that the accuracy of the low-precision studies is lower than it is possible to judge from the individual studies themselves. Some possible sources of systematic error have been discussed. The effect of an improper choice of scattering length for D in not fully deuterated samples has been demonstrated.

The most precise and accurate observations of vibrational amplitudes made by neutron diffraction have been shown to be in good agreement with results from vibrational spectroscopy. The combination of neutron-diffraction results and experience from spectroscopic work give more comprehensive information about the form of the normal vibrations, especially the water librations.

The hydrogen-bond strength correlates to the librational amplitudes of the water molecule; the stronger the bond, the smaller the amplitudes. The vibrational amplitudes of the O nucleus of the water molecule depend on the coordination type so that a more anisotropic vibrational behaviour is found for class 1 molecules.

Even if the diffraction measurements and processing techniques have improved during the last decade, it is clear that the reliability of the diffraction-obtained vibrational parameters is in many cases far from satisfactory. In spite of this, it would seem that the enormous wealth of accumulated diffraction data should be used more often in solving problems related to vibrations in crystals.

We are grateful to Drs G. Chiari and G. Ferraris, University of Torino, Italy, who sent us their survey of water molecules prior to publication. The Executive Secretary of the IUCr and a number of other persons have kindly provided us with unpublished thermal parameters. This study has been supported by grants from the Swedish Natural Science Research Council.

References

Berglund, B., Lindgren, J. & Tegenfeldt, J. (1978). *J. Mol. Struct.* **43**, 169–177.
Chiari, G. & Ferraris, G. (1982). *Acta Cryst.* B**38**, 2331–2341.
Eriksson, A., Berglund, B., Tegenfeldt, J. & Lindgren, J. (1979). *J. Mol. Struct.* **52**, 107–112.
Eriksson, A., Hermansson, K., Lindgren, J. & Thomas, J. O. (1982). *Acta Cryst.* A**38**, 138–142.
Eriksson, A. & Lindgren, J. (1978*a*). *J. Mol. Struct.* **48**, 417–430.
Eriksson, A. & Lindgren, J. (1978*b*). *Acta Chem. Scand. Ser. A*, **32**, 737–746.
Falk, M. & Knop, O. (1973). *Water – A Comprehensive Treatise*, Vol. 2, ch. 2, edited by F. Franks. New York: Plenum.
Ferraris, G. & Franchini-Angela, M. (1972). *Acta Cryst.* B**28**, 3572–3583.
Hamilton, W. C. & Abrahams, S. C. (1970). *Acta Cryst.* A**26**, 18–24.
Hermansson, K. (1983). *Acta Cryst.* C**39**, 925–930.
Hermansson, K. & Thomas, J. O. (1982). *Acta Cryst.* B**38**, 2555–2563.
Hirshfeld, F. L. (1976). *Acta Cryst.* A**32**, 239–244.
Ichida, K., Kuroda, Y., Nakamura, D. & Kubo, M. (1972). *Spectrochim. Acta Part A*, **28**, 2433–2441.
Pedersen, B. (1975). *Acta Cryst.* B**31**, 874–879.
Rosenfield, R. E., Trueblood, K. N. & Dunitz, J. D. (1978). *Acta Cryst.* A**34**, 828–829.
Tellgren, R., Thomas, J. O. & Olovsson, I. (1977). B**33**, 3500–3504.
Thomas, G. H., Falk, M. & Knop, O. (1974). *Can. J. Chem.* **52**, 1029–1041.
Trueblood, K. N. & Dunitz, J. D. (1983). *Acta Cryst.* B**39**, 120–133.
Willis, B. T. M. & Howard, J. A. K. (1975). *Acta Cryst.* A**31**, 514–520.

Acta Cryst. (1983). B**39**, 711–717

cis-Bis(bipyridyl)dichloroiron(III) Tetrachloroferrate(III), $[Fe(bpy)_2Cl_2][FeCl_4]$; Structure at 4·2 and at 115 K by Neutron Diffraction

By Brian N. Figgis and Philip A. Reynolds

School of Chemistry, The University of Western Australia, Nedlands, WA 6009, Australia

and Norbert Lehner

Institut Laue–Langevin, 156X, Centre de Tri, 38042 Grenoble CEDEX, France

(*Received* 20 *April* 1983; *accepted* 5 *July* 1983)

Abstract

The crystal structure of deuterated *cis*-$[Fe^{III}(bpy)_2Cl_2]$ $[Fe^{III}Cl_4]$ has been determined by single-crystal neutron diffraction methods at 4·2 K. Crystals are orthorhombic, *Pccn*. At 4·2 K $a = 14{\cdot}97\,(1)$, $b = 12{\cdot}21\,(1)$, $c = 13{\cdot}26\,(2)$ Å. Refinement of all 2895 measured unique reflections with anisotropic thermal motion [220 parameters (nv)] converged to $R(F^2) = 0{\cdot}050$, $\chi = 2{\cdot}6$. In addition, 869 reflections were measured at 115 K on the deuterated crystal and 426 reflections at 4·2 K on a hydrogenous crystal. These sets have low resolution in *b* and the refinements were constrained accordingly. These converged to $R(F^2) = 0{\cdot}060$, $\chi = 1{\cdot}4$, nv = 195 and $R(F^2) = 0{\cdot}062$, $\chi = 3{\cdot}8$, nv = 145. From these results the geometry, and the temperature and isotopic dependence of U_{11}, U_{33} and U_{13} were obtained. The crystal structure closely resembles that determined by X-ray diffraction at 295 K, but with precision better by a factor of three. This improvement allows a small distortion in the bipyridyl ligand to be defined. The thermal motion of the H and D atoms clearly shows the effect of zero-point *intramolecular* motion at 4·2 K. With that correction, the thermal parameters increase fairly uniformly over the atoms by a factor of three between 4·2 and 115 K, corresponding to a crystal Debye temperature of *ca* 115 K.

Introduction

The effects of covalency can be studied by using the technique of polarized neutron diffraction (p.n.d.). A number of simple molecules and ions have been studied by this method – for example, $CoCl_4^{2-}$ (Chandler, Figgis, Phillips, Reynolds, Mason & Williams, 1982), $CoBr_4^{2-}$ (Figgis, Reynolds & Mason, 1982), $Ni(ND_3)_4(NO_2)_2$ (Figgis, Reynolds & Mason, 1983), and manganese phthalocyanine (Figgis, Williams, Forsyth & Mason, 1981). In this work we investigate an oxidation state higher than two with polarizable ligands so as to increase the likely effects of covalency. We selected the dimeric adduct of bipyridyl with $FeCl_3$ (Figgis, Patrick, Reynolds, Skelton, White & Healy, 1983) since this provides information on both tetrahedral Fe^{III} (in the $FeCl_4^-$ anion) and octahedral Fe^{III} [in the $Fe(bpy)_2Cl_2^+$ cation]. A prerequisite of the p.n.d. experiment is the conventional neutron diffraction structural experiment at 4·2 K, preferably on perdeuterated material which we present and analyse here. Since such structures determined at 4·2 K are, as yet, uncommon we also performed some, more limited, experiments at 115 K, and at 4·2 K on the hydrogenous material, which results are also presented. These illustrate the effects of isotopic substitution and zero-point motion at low temperatures. They may also be useful in connection with the charge density study by X-ray diffraction which we also have in hand. The results of the p.n.d. experiment which we carried out subsequent to the present work will be reported separately.

Experimental

Deuterated bipyridyl was produced by heating 1 g of bipyridyl with 5 g 99% deuterated water and 0·1 g MgO in a sealed tube at 600 K for 24 h. The tube was broken, the water evaporated, and the residue again exchanged with 5 g 99% deuterated water. The deuterated bipyridyl was recrystallized from ethanol. The degree of deuteration was measured by mass spectrometry and NMR as 90 (2)%. Anhydrous ferric chloride was dissolved in nitromethane with a stoichiometric amount of deuterated bipyridyl, the solution was filtered and allowed to evaporate slowly, giving large crystals. The crystal morphology (well developed {100}, {102}, {010}, less well developed {110}, {112}) and the X-ray diffraction patterns of chips broken off showed them to be $[Fe^{III}(bpy)_2Cl_2][Fe^{III}Cl_4]$, isomorphous with the hydrogenous complex (Figgis, Patrick *et al.*, 1983).

Neutron diffraction intensities were obtained with a wavelength of 1·176 Å on the D15 normal-beam diffractometer with motorized lifting counter at the Institut Laue–Langevin, Grenoble. Four data sets were obtained in all. An 18 mm³ crystal of the hydrogenous complex was mounted with *b* vertical and 426 unique reflections measured at 4·2 K with $\sin\theta/\lambda \le 0{\cdot}74$ Å^{-1} *via* an ω scan (set *A*). An 11 mm³ deuterated crystal was mounted with *c* vertical and 1303 reflections measured at 4·2 K (set *B*). In addition, several reflections equivalent and/or absent in *Pccn* were measured. The data showed good orthorhombic equivalence, but significant, although small, forbidden reflections, which may be attributable to multiple scattering. Accordingly, to minimize this effect a smaller (6 mm³) crystal was mounted with *b* 5° displaced from the vertical in both *a* and *c*. 1592 reflections were measured at 4·2 K (set *c*) and a further 869 at 115 K (set *D*). In all cases, the strongest reflection, 600, was measured every 50 reflections as a standard. No significant variation in this standard intensity was observed in each data set. Integrated intensities were obtained by use of the profile-analysis program *COLL*5 (Lehmann & Wilson, 1979). The path lengths for scattered neutrons were in all cases 3 to 4 mm. For data sets *A*, *C* and *D* it was possible to select crystals with small cross sections in the scattering plane. We estimated that the absorption together with the incoherent scattering gives cross sections of 0·03 and 0·13 mm^{-1} for the deuterated and the hydrogenous materials respectively. We considered that an absorption correction was unnecessary. For each data set unit-cell parameters were obtained by a least-squares analysis of the setting angles of from 10 to 15 reflections well separated in diffractometer angles and are listed in Table 1. Apart from slight restrictions due to the cryostat blind spots, the main limitation in an individual data set arises from the small available range in the lifting-counter angle, ν. This causes resolution in the diffractometer vertical direction to be restricted to $\sin\theta/\lambda \le 0{\cdot}210$ Å^{-1}. By combination of sets *B* and *C*

Table 1. *Cell dimensions of various crystals* (Å)

N: neutron diffraction, *X*: X-ray diffraction, H: hydrogenous crystal, and D: deuterated crystal.

Set	Technique	Crystal	*T*(K)	*a*	*b*	*c*
A	*N*	H	4·2	14·92 (4)	12·16 (4)	13·22 (5)
B	*N*	D	4·2	14·97 (2)	12·24 (2)	13·21 (2)
C	*N*	D	4·2	14·970 (5)	12·18 (2)	13·270 (5)
D	*N*	D	115 (2)	15·02 (2)	12·26 (2)	13·35 (1)
—	*X**	D	120 (3)	14·996 (7)	12·325 (6)	13·336 (5)
—	*X**	D	295	15·013 (5)	12·474 (5)	13·516 (5)
—	*X*†	H	295	15·013 (4)	12·471 (3)	13·510 (5)

* Figgis *et al.* (unpublished data).
† Figgis, Patrick *et al.* (1983).

a truly three-dimensional data set can be obtained for the deuterated material at 4·2 K. However, both set *A* and set *D* have limited resolution in the *k* reciprocal direction. The mean F^2 of the reflections formally forbidden in *Pccn* fell from 0·008 of $F^2(600)$ to 0·002 from set *B* to set *C*. This indicates that multiple scattering is small, but significant, and that the space group at 4·2 K has absences consistent with *Pccn* (0*kl* and *h*0*l*, *l* odd absent, and *hk*0, $h+k$ odd absent). To provide a crude multiple-scattering correction the respective mean F^2's of the measured absent reflections were subtracted from sets *B* and *C* (Le Page & Gabe, 1979). Sets *A* and *D* seem less affected by multiple scattering.

Refinement

Structure refinements were performed using the XRAY76 system (Stewart, Machin, Dickinson, Ammon, Heck & Flack, 1976). In all cases the function $\sum w(F_o^2 - F_c^2)^2$ was minimized using all data, with no rejection criterion, and weighting $w = \sigma(F_o^2)^{-2}$. Initially the four data sets *A*–*D* were fitted by a refinement of nuclear coordinates, isotropic temperature factor and extinction coefficient, and a scale factor. Starting coordinates were taken from Figgis, Patrick *et al.* (1983) and scattering lengths from Koester (1977). In addition, for sets *B*–*D* the 'deuterium' scattering length was also refined so as to estimate the percentage deuteration. The refinements were then allowed to become anisotropic using temperature factors of the form $\exp[-2\pi^2(U_{11}h^2a^{*2} + \ldots + 2U_{23}klb^*c^*)]$. Due to the limited resolution in one dimension the refinements were constrained. For sets *A*, *C* and *D* U_{12} and U_{23} were kept at zero, and U_{22} at the isotropic value; for set *B* U_{13} and U_{23} were kept at zero, and U_{33} at the isotropic value. Allowing the off-diagonal elements U_{12}, U_{23} and U_{13} to refine produced no significant improvement for sets *A*, *B* and *C*. The refined values for the badly defined elements (U_{12} and U_{23} or U_{13} and U_{23}) differed from zero by less than 2σ ($\sigma \sim 18$ pm^2 typically). For set *D* there was a significant improvement in refining U_{12} and U_{23}. This is not unexpected given the larger values expected for the off-diagonal elements at this higher temperature of 115 K. The final refined values for χ $\{= [\sum w(F_o^2 - F_c^2)/(\text{no} - \text{nv})]^{1/2}\}$, *R*, number of observations (no), number of variables (nv) for the four sets are: (*A*) 3·8, 0·062, 426, 146; (*B*) 2·9, 0·042, 1303, 149; (*C*) 2·2, 0·060, 1592, 147; (*D*) 1·4, 0·060, 869, 195. Nuclear positional and thermal parameters from these refinements are given in Table 2.* Fe(2), Cl(21) and Cl(22) compose the $FeCl_4^-$ anion, while Fe(1), Cl(11), N(11) to C(16), and N(22) to C(26) compose the cation with the two independent pyridine rings N(11) to C(16) and N(21) to C(26) linked through the bond C(12)–C(22). The scattering length of the deuterium site corresponded to 91·1 (3), 89·0 (3), and 90·1 (3)% deuteration from sets *B* to *D* respectively. The extinction parameter was in all cases small, negligible for sets *A* and *C* and giving a *maximum* reduction in F^2 of 8% for set *B* and 4% for *D*. Since *C* and *D* are the same crystal with set *D* the later measurement, extinction in *C* would be likely to be greater than in *D*. We therefore ascribe the apparent extinction to errors in the measurement of a very few intense reflections. Perusal of Table 2 shows that values of *x*,*y*,*z*, and U_{11}, which are well determined by both sets *B* and *C*, are not significantly different in the refinements of the two sets. Extinction is small enough to neglect, and as the degree of deuteration is the same (since the crystals derive from the same batch) we refined sets *B* and *C* together with no constraints, the data then being three-dimensional. The resulting refinement, which we call *B* + *C*, gave $\chi = 2{\cdot}6$, $R = 0{\cdot}050$ for no = 2895, nv = 220 with a final maximum parameter shift to error of 0·11. The nuclear positional and thermal parameters for this refinement are also listed in Table 2.* The refined percentage deuteration was 90·0 (2)%. Allowing crystallographically distinct deuteriums to have independent scattering lengths produced no significant improvement, showing uniform deuteration of the bipyridyl hydrogens. A refinement in which $\sum \| F_o| - |F_c\|^2$ was minimized, and those reflections in which $F^2 \leq 3\sigma(F^2)$ were rejected gave parameter values not significantly different from above with a residual $R = 0{\cdot}032$, no = 2294.

---

* Lists of structure factors (sets *A*, *B*, *C*, *D*, and *B* + *C*) have been deposited with the British Library Lending Division as Supplementary Publication No. SUP 38723 (25 pp.). Copies may be obtained through The Executive Secretary, International Union of Crystallography, 5 Abbey Square, Chester CH1 2HU, England.

Table 2. *Atomic positional coordinates* (×10^4) *and thermal parameters* (Å^2 × 10^4)

Set *A* is hydrogenous at 4·2 K, *B* and *C* are deuterated at 4·2 K, *D* is deuterated at 115 K. A dashed e.s.d. implies no refinement of that parameter.

	Set	x	y	z	U_{11}	U_{22}	U_{33}	U_{12}	U_{13}	U_{23}
Fe(1)	*A*	2500	2500	2304 (3)	72 (10)	102 (–)	122 (19)	0 (–)	0	0
	B	2500	2500	2304 (4)	43 (5)	24 (5)	30 (–)	6 (4)	0	0
	C	2500	2500	2300 (1)	49 (5)	55 (–)	54 (5)	0 (–)	0	0
	D	2500	2500	2302 (1)	120 (5)	120 (–)	147 (6)	20 (10)	0	0
	B + *C*	2500	2500	2301 (1)	44 (4)	22 (4)	59 (5)	5 (4)	0	0
Fe(2)	*A*	7500	2500	975 (4)	71 (9)	115 (–)	175 (21)	0 (–)	0	0
	B	7500	2500-	978 (4)	58 (5)	54 (5)	55 (–)	–16 (4)	0	0
	C	7500	2500	980 (1)	59 (6)	63 (–)	70 (5)	0 (–)	0	0
	D	7500	2500	966 (1)	216 (7)	206 (–)	212 (7)	–54 (13)	0	0
	B + *C*	7500	2500	981 (1)	56 (4)	54 (4)	71 (6)	–13 (4)	0	0
Cl(11)	*A*	1577 (1)	1672 (6)	1205 (2)	100 (7)	92 (–)	96 (12)	0 (–)	22 (7)	0 (–)
	B	1576 (1)	1658 (1)	1191 (2)	71 (4)	53 (3)	64 (–)	0 (4)	0 (–)	0 (–)
	C	1576 (1)	1659 (2)	1199 (1)	80 (4)	77 (–)	73 (3)	0 (–)	–23 (3)	0 (–)
	D	1580 (1)	1660 (2)	1206 (1)	222 (5)	220 (–)	228 (5)	–7 (8)	–70 (4)	–25 (7)
	B + *C*	1576 (1)	1658 (1)	1199 (1)	72 (3)	45 (3)	78 (4)	3 (3)	–21 (3)	–13 (5)
Cl(21)	*A*	8086 (2)	1217 (6)	27 (2)	112 (7)	120 (–)	100 (13)	0 (–)	13 (8)	0 (–)
	B	8085 (1)	1218 (1)	22 (3)	91 (4)	91 (4)	92 (–)	–23 (3)	0 (–)	0 (–)
	C	8087 (1)	1221 (2)	16 (1)	107 (5)	108 (–)	106 (4)	0 (–)	28 (3)	0 (–)
	D	8085 (1)	1228 (3)	10 (1)	344 (6)	370 (–)	431 (8)	–146 (11)	120 (6)	–257 (10)
	B + *C*	8084 (1)	1218 (1)	16 (1)	90 (3)	86 (3)	110 (4)	–21 (3)	27 (3)	–41 (5)
Cl(22)	*A*	6484 (2)	1689 (6)	1914 (3)	108 (7)	114 (–)	121 (17)	0 (–)	27 (9)	0 (–)
	B	6481 (1)	1688 (1)	1915 (2)	75 (4)	52 (4)	59 (–)	–10 (3)	0 (–)	0 (–)
	C	6480 (1)	1685 (2)	1912 (1)	77 (4)	83 (–)	91 (4)	0 (–)	9 (3)	0 (–)
	D	6480 (1)	1704 (3)	1889 (1)	249 (5)	243 (–)	265 (6)	–57 (8)	51 (4)	–1 (8)
	B + *C*	6481 (1)	1689 (1)	1912 (1)	70 (3)	51 (3)	91 (4)	–9 (3)	10 (3)	4 (5)
N(11)	*A*	1593 (2)	2077 (7)	3509 (3)	82 (8)	87 (–)	101 (16)	0 (–)	24 (8)	0 (–)
	B	1592 (1)	2069 (1)	3513 (2)	51 (4)	38 (4)	45 (–)	0 (4)	0 (–)	0 (–)
	C	1591 (1)	2067 (2)	3512 (1)	57 (4)	68 (–)	69 (4)	0 (–)	5 (3)	0 (–)
	D	1596 (1)	2064 (2)	3509 (1)	142 (5)	154 (–)	175 (5)	–16 (8)	11 (4)	24 (7)
	B + *C*	1591 (1)	2069 (1)	3512 (1)	47 (3)	32 (3)	69 (4)	1 (3)	7 (3)	10 (4)
N(21)	*A*	1692 (1)	3916 (6)	2527 (3)	99 (8)	111 (–)	105 (14)	0 (–)	–9 (9)	0 (–)
	B	1686 (1)	3926 (1)	2534 (2)	53 (4)	30 (4)	37 (–)	15 (3)	0 (–)	0 (–)
	C	1685 (1)	3921 (2)	2530 (1)	49 (4)	63 (–)	67 (4)	0 (–)	5 (3)	0 (–)
	D	1684 (1)	3910 (2)	2529 (1)	150 (5)	168 (–)	186 (5)	33 (8)	–4 (4)	–15 (7)
	B + *C*	1686 (1)	3925 (1)	2530 (1)	52 (3)	24 (3)	62 (4)	13 (3)	5 (3)	–2 (5)
C(12)	*A*	912 (2)	2737 (9)	3681 (4)	69 (11)	97 (–)	168 (20)	0 (–)	16 (12)	0 (–)
	B	908 (1)	2763 (1)	3683 (3)	67 (5)	44 (5)	57 (–)	7 (5)	0 (–)	0 (–)
	C	912 (1)	2768 (3)	3681 (1)	52 (6)	67 (–)	72 (5)	0 (–)	2 (4)	0 (–)
	D	918 (1)	2756 (3)	3682 (1)	128 (6)	154 (–)	187 (7)	–35 (11)	14 (5)	–46 (9)
	B + *C*	908 (1)	2764 (1)	3682 (1)	59 (4)	40 (4)	65 (6)	4 (4)	6 (4)	13 (6)
C(13)	*A*	237 (3)	2516 (14)	4374 (8)	101 (13)	138 (–)	197 (40)	0 (–)	42 (14)	0 (–)
	B	235 (1)	2526 (1)	4361 (4)	73 (6)	84 (6)	74 (–)	–9 (5)	0 (–)	0 (–)
	C	240 (1)	2524 (3)	4371 (1)	57 (6)	89 (–)	113 (5)	0 (–)	27 (5)	0 (–)
	D	246 (1)	2520 (4)	4369 (2)	185 (7)	234 (–)	267 (8)	–62 (14)	74 (6)	–62 (13)
	B + *C*	236 (1)	2526 (1)	4368 (1)	66 (4)	76 (5)	106 (6)	–6 (4)	26 (5)	1 (6)
C(14)	*A*	274 (2)	1549 (11)	4899 (4)	133 (13)	166 (–)	105 (26)	0 (–)	22 (12)	0 (–)
	B	283 (1)	1552 (1)	4923 (4)	86 (6)	78 (6)	79 (–)	–25 (5)	0 (–)	0 (–)
	C	283 (1)	1549 (3)	4911 (1)	83 (6)	90 (–)	96 (5)	0 (–)	20 (5)	0 (–)
	D	291 (1)	1550 (4)	4900 (2)	301 (9)	250 (–)	250 (8)	–136 (15)	93 (7)	–52 (14)
	B + *C*	282 (1)	1550 (1)	4912 (1)	93 (4)	71 (5)	87 (6)	–29 (4)	27 (5)	4 (7)
C(15)	*A*	984 (2)	854 (8)	4726 (4)	133 (12)	129 (–)	135 (21)	0 (–)	40 (13)	0 (–)
	B	989 (1)	843 (1)	4729 (4)	110 (6)	57 (6)	79 (–)	–16 (5)	0 (–)	0 (–)
	C	991 (1)	848 (3)	4733 (1)	104 (7)	93 (–)	80 (5)	0 (–)	4 (5)	0 (–)
	D	995 (1)	841 (4)	4725 (1)	337 (10)	248 (–)	190 (7)	–110 (13)	19 (7)	26 (15)
	B + *C*	989 (1)	843 (1)	4734 (1)	106 (4)	51 (5)	79 (6)	–18 (4)	4 (5)	–8 (7)
C(16)	*A*	1627 (2)	1126 (9)	4026 (4)	79 (13)	122 (–)	167 (19)	0 (–)	41 (12)	0 (–)
	B	1630 (1)	1127 (1)	4038 (4)	83 (6)	56 (5)	65 (–)	–4 (5)	0 (–)	0 (–)
	C	1631 (1)	1129 (3)	4026 (1)	86 (7)	89 (–)	91 (5)	0 (–)	19 (4)	0 (–)
	D	1635 (1)	1126 (4)	4019 (1)	231 (8)	202 (–)	215 (8)	–41 (13)	12 (6)	26 (11)
	B + *C*	1630 (1)	1126 (1)	4027 (1)	82 (4)	50 (5)	94 (6)	–3 (4)	12 (5)	13 (7)
C(22)	*A*	*966 (2)*	*3799 (7)*	*3114 (4)*	*65 (10)*	*95 (–)*	*87 (17)*	*0 (–)*	*–13 (10)*	*0 (–)*
	B	958 (1)	3804 (1)	3111 (3)	65 (5)	36 (5)	53 (–)	12 (5)	0 (–)	0 (–)
	C	958 (1)	3806 (3)	3120 (1)	52 (6)	75 (–)	86 (5)	0 (–)	–8 (4)	0 (–)
	D	958 (1)	3799 (4)	3125 (1)	126 (7)	178 (–)	210 (8)	31 (11)	–13 (5)	–33 (10)
	B + *C*	957 (1)	3803 (1)	3120 (1)	57 (4)	34 (5)	79 (6)	12 (4)	–3 (5)	–9 (7)
C(23)	*A*	323 (2)	4632 (8)	3211 (4)	77 (13)	121 (–)	173 (22)	0 (–)	–5 (13)	0 (–)
	B	320 (1)	4627 (1)	3211 (3)	60 (6)	64 (6)	62 (–)	30 (5)	0 (–)	0 (–)
	C	322 (1)	4622 (3)	3206 (1)	58 (6)	86 (–)	110 (6)	0 (–)	14 (5)	0 (–)
	D	324 (1)	4614 (4)	3213 (2)	164 (8)	250 (–)	358 (10)	93 (12)	–14 (7)	–42 (14)
	B + *C*	319 (1)	4628 (1)	3208 (1)	65 (4)	54 (5)	104 (6)	31 (4)	13 (5)	5 (7)
C(24)	*A*	449 (3)	5612 (9)	2691 (4)	120 (12)	142 (–)	183 (21)	0 (–)	11 (13)	0 (–)
	B	454 (1)	5605 (1)	2686 (3)	82 (5)	63 (6)	67 (–)	33 (5)	0 (–)	0 (–)
	C	452 (1)	5608 (3)	2692 (1)	95 (6)	97 (–)	98 (5)	0 (–)	4 (5)	0 (–)
	D	450 (1)	5577 (5)	2699 (2)	231 (9)	306 (–)	400 (11)	145 (17)	–47 (8)	–64 (15)
	B + *C*	454 (1)	5606 (1)	2691 (1)	89 (4)	58 (5)	97 (6)	32 (4)	–6 (5)	7 (7)

Table 2 (*cont.*)

	Set	x	y	z	U_{11}	U_{22}	U_{33}	U_{12}	U_{13}	U_{23}
C(25)	A	1212 (2)	5743 (9)	2107 (4)	128 (12)	119 (–)	102 (19)	0 (–)	–38 (12)	0 (–)
	B	1212 (1)	5730 (1)	2103 (3)	90 (6)	43 (5)	58 (–)	15 (5)	0 (–)	0 (–)
	C	1213 (1)	5729 (3)	2106 (1)	96 (7)	93 (–)	99 (5)	0 (–)	–5 (5)	0 (–)
	D	1206 (1)	5712 (4)	2116 (2)	296 (10)	273 (–)	273 (9)	102 (16)	–61 (8)	–36 (15)
	$B + C$	1212 (1)	5731 (1)	2106 (1)	75 (4)	35 (5)	106 (6)	16 (4)	–8 (5)	–5 (7)
C(26)	A	1814 (2)	4867 (8)	2045 (4)	108 (12)	109 (–)	99 (19)	0 (–)	20 (13)	0 (–)
	B	1816 (1)	4872 (1)	2031 (3)	58 (6)	40 (5)	52 (–)	10 (4)	0 (–)	0 (–)
	C	1810 (1)	4880 (3)	2037 (1)	51 (6)	78 (–)	92 (5)	0 (–)	13 (4)	0 (–)
	D	1804 (1)	4857 (4)	2042 (1)	212 (8)	204 (–)	231 (8)	23 (12)	–17 (6)	16 (12)
	$B + C$	1815 (1)	4874 (1)	2035 (1)	58 (4)	32 (4)	87 (6)	13 (4)	10 (5)	22 (7)
H(13)	A	–310 (6)	3098 (17)	4498 (8)	276 (36)	258 (–)	201 (52)	0 (–)	58 (28)	0 (–)
	B	–303 (1)	3090 (2)	4504 (4)	177 (9)	175 (8)	176 (–)	28 (7)	0 (–)	0 (–)
	C	–308 (1)	3081 (4)	4502 (2)	128 (10)	178 (–)	231 (10)	0 (–)	54 (7)	0 (–)
	D	–293 (2)	3076 (6)	4505 (2)	298 (12)	383 (–)	533 (17)	–2 (23)	175 (11)	–82 (21)
	$B + C$	–304 (1)	3087 (2)	4504 (2)	156 (7)	165 (7)	223 (10)	19 (6)	62 (7)	–8 (10)
H(14)	A	–223 (7)	1427 (33)	5445 (18)	269 (31)	281 (–)	291 (93)	0 (–)	113 (38)	0 (–)
	B	–221 (1)	1369 (2)	5477 (5)	186 (10)	209 (10)	182 (–)	–39 (8)	0 (–)	0 (–)
	C	–217 (2)	1376 (4)	5475 (2)	217 (12)	174 (–)	181 (9)	0 (–)	100 (8)	0 (–)
	D	–210 (2)	1372 (7)	5467 (2)	502 (16)	373 (–)	431 (16)	–149 (27)	236 (12)	–17 (25)
	$B + C$	–223 (1)	1372 (2)	5473 (2)	184 (7)	193 (8)	188 (10)	–33 (7)	99 (8)	28 (10)
H(15)	A	1068 (8)	86 (19)	5180 (8)	343 (36)	297 (–)	209 (47)	0 (–)	–43 (34)	0 (–)
	B	1062 (2)	82 (2)	5143 (5)	261 (10)	149 (9)	199 (–)	–11 (8)	0 (–)	0 (–)
	C	1061 (2)	74 (5)	5144 (2)	223 (11)	193 (–)	176 (9)	0 (–)	27 (8)	0 (–)
	D	1070 (3)	76 (7)	5122 (2)	555 (19)	454 (–)	347 (14)	–214 (23)	29 (12)	124 (26)
	$B + C$	1063 (1)	83 (2)	5146 (2)	248 (7)	140 (8)	177 (10)	–14 (6)	29 (8)	56 (11)
H(16)	A	2184 (6)	652 (21)	3857 (9)	208 (28)	247 (–)	391 (63)	0 (–)	118 (36)	0 (–)
	B	2188 (2)	595 (2)	3872 (4)	182 (9)	140 (8)	154 (–)	53 (7)	0 (–)	0 (–)
	C	2191 (2)	586 (4)	3873 (2)	159 (9)	171 (–)	192 (9)	0 (–)	38 (8)	0 (–)
	D	2190 (2)	593 (6)	3857 (2)	340 (13)	383 (→)	435 (15)	38 (20)	70 (12)	106 (21)
	$B + C$	2190 (1)	596 (2)	3872 (2)	169 (6)	132 (7)	196 (9)	54 (6)	51 (8)	55 (11)
H(23)	A	–269 (5)	4480 (21)	3665 (10)	218 (28)	302 (–)	364 (58)	0 (–)	128 (36)	0 (–)
	B	–261 (1)	4523 (2)	3667 (5)	150 (9)	210 (9)	165 (–)	31 (8)	0 (–)	0 (–)
	C	–268 (2)	4524 (4)	3675 (2)	125 (9)	162 (–)	199 (9)	0 (–)	75 (7)	0 (–)
	D	–262 (2)	4497 (6)	3680 (3)	253 (11)	394 (–)	601 (20)	126 (19)	122 (12)	–57 (22)
	$B + C$	–264 (1)	4524 (2)	3674 (2)	140 (6)	197 (8)	193 (10)	37 (6)	76 (7)	35 (10)
H(24)	A	–40 (6)	6265 (24)	2757 (8)	262 (37)	276 (–)	283 (50)	0 (–)	13 (34)	0 (–)
	B	–40 (2)	6253 (2)	2764 (5)	199 (9)	181 (9)	181 (–)	100 (8)	0 (–)	0 (–)
	C	–39 (2)	6254 (5)	2765 (2)	158 (10)	212 (–)	262 (10)	0 (–)	45 (8)	0 (–)
	D	–35 (2)	6235 (8)	2778 (3)	431 (16)	518 (–)	683 (25)	265 (29)	14 (16)	–35 (25)
	$B + C$	–37 (1)	6251 (2)	2767 (2)	179 (7)	162 (8)	270 (11)	97 (7)	48 (8)	32 (11)
H(25)	A	1378 (6)	6495 (22)	1694 (10)	272 (34)	346 (–)	311 (60)	0 (–)	25 (37)	0 (–)
	B	1349 (2)	6481 (2)	1699 (5)	230 (10)	115 (9)	179 (–)	16 (7)	0 (–)	0 (–)
	C	1351 (2)	6491 (5)	1710 (2)	206 (11)	199 (–)	213 (10)	0 (–)	22 (8)	0 (–)
	D	1345 (3)	6456 (7)	1717 (3)	480 (17)	428 (–)	453 (16)	108 (26)	–53 (13)	60 (27)
	$B + C$	1350 (1)	6482 (2)	1709 (2)	209 (7)	102 (8)	231 (10)	19 (6)	21 (8)	62 (11)
H(26)	A	2415 (6)	4922 (15)	1591 (7)	285 (29)	273 (–)	219 (35)	0 (–)	106 (32)	0 (–)
	B	2408 (1)	4928 (2)	1578 (5)	160 (9)	151 (8)	151 (–)	3 (7)	0 (–)	0 (–)
	C	2413 (2)	4921 (4)	1583 (2)	115 (10)	165 (–)	193 (8)	0 (–)	77 (7)	0 (–)
	D	2399 (2)	4920 (7)	1589 (2)	341 (12)	357 (–)	374 (12)	32 (19)	82 (10)	60 (21)
	$B + C$	2409 (1)	4926 (2)	1584 (2)	139 (6)	144 (7)	185 (8)	5 (6)	67 (7)	45 (11)

Discussion

Intramolecular geometry

The crystal is composed of *cis*-$[\mathrm{Fe^{III}(bpy)_2Cl_2}]^+$ cations and $[\mathrm{Fe^{III}Cl_4}]^-$ anions which are illustrated in Figs. 1 and 2 respectively. The Fe atoms of each species lie on a twofold axis. The Fe-atom environments are respectively approximately octahedral and tetrahedral. The bond lengths and angles are listed in Table 3 for the $B + C$ 4·2 K neutron refinement and the 295 K X-ray refinement (Figgis, Patrick *et al.*, 1983). The bipyridyl-ligand geometry is given in Table 4. The rather unsymmetrical and distorted Fe-atom environments have been fully discussed elsewhere (Figgis, Patrick *et al.*, 1983). In the context of the molecular geometry, note the increased precision of this experiment – a factor of at least three. This, while partly due to the use of neutron diffraction (constant form factors, no valence effects), is mainly due to the small thermal parameters at 4·2 K compared to 295 K (approximately a tenfold reduction in size). This also obviates the need for thermal correction of the bond lengths. Around the Fe atom in $\mathrm{FeCl_4^-}$ the apparent bond lengths increase from 295 to 4·2 K. This may be due to apparent bond shortening at 295 K by the large librational motion of the $\mathrm{FeCl_4^-}$ anion or to valence effects on the X-ray data. This apparent bond shortening at 295 K is also apparent in the bipyridyl ligand, the mean C—C ring bond length increasing from 1·374 to 1·389 Å between 295 and 4·2 K. The increased precision of this experiment relative to the 295 K X-ray structure, or indeed *any* other previous structure containing bipyridyl, shows some interesting distortions in the bipyridyl ligand. All ring C—C, C—N and the C—D bond lengths are not significantly

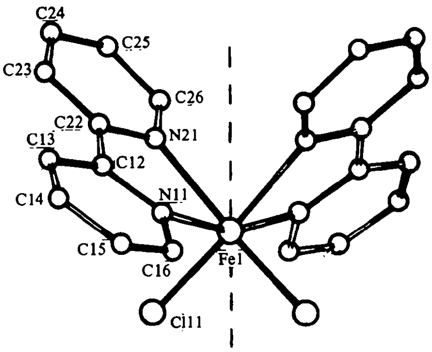

Fig. 1. The *cis*-bis(bipyridyl)dichloroiron(III) cation, with the twofold axis, *c*, indicated.

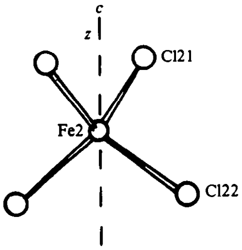

Fig. 2. The tetrachloroferrate(III) anion, with the twofold axis, *c*, indicated.

Table 3. Fe-*atom environment: neutron* 4·2 K *results are the first entry*, 295 K *X-ray the second*

Cation $[Fe(bpy)_2Cl_2]^+$

	r_{FeX} (Å)	N(11) (°)	N(21) (°)	Cl(11) (°)	N(11) (°)	N(21) (°)
Cl(11)	2·260 (2)	89·1 (1)	96·5 (1)	99·5 (1)	166·6 (1)	94·0 (1)
	2·254 (2)	89·0 (1)	96·5 (1)	99·6 (1)	166·9 (1)	94·3 (1)
N(11)	2·170 (2)		74·7 (1)		84·5 (1)	93·1 (1)
	2·174 (4)		74·9 (1)		84·3 (1)	92·7 (1)
N(21)	2·146 (2)					163·7 (1)
	2·144 (4)					163·1 (1)

Anion $[FeCl_4]^-$

	r_{FeCl} (Å)	Cl(22) (°)	Cl(21) (°)	Cl(22) (°)
Cl(21)	2·203 (2)	106·4 (1)	109·0 (1)	111·8 (1)
	2·190 (2)	106·8 (1)	110·2 (1)	110·9 (1)
Cl(22)	2·198 (2)			113·7 (1)
	2·185 (2)			111·3 (1)

Table 4. *Distances* (Å) *and angles* (°) *involving the bipyridyl ligand*

4·2 K neutron data are given first, 295 K X-ray data second (for non-hydrogen bonds).

N(11)–C(12)	1·347 (2)	N(21)–C(22)	1·351 (2)
	1·346 (6)		1·353 (6)
C(12)–C(13)	1·388 (2)	C(22)–C(23)	1·392 (2)
	1·375 (8)		1·388 (8)
C(13)–C(14)	1·396 (2)	C(23)–C(24)	1·391 (2)
	1·367 (10)		1·380 (9)
C(14)–C(15)	1·385 (2)	C(24)–C(25)	1·384 (2)
	1·357 (10)		1·362 (10)
C(15)–C(16)	1·385 (2)	C(25)–C(26)	1·384 (2)
	1·377 (8)		1·386 (8)
C(16)–N(11)	1·341 (2)	C(26)–N(21)	1·346 (2)
	1·337 (7)		1·344 (6)
C(12)–C(22)	1·473 (2)		
	1·461 (7)		
C(13)–H(13)	1·075 (2)	C(23)–H(23)	1·078 (2)
C(14)–H(14)	1·083 (3)	C(24)–H(24)	1·082 (2)
C(15)–H(15)	1·083 (3)	C(25)–H(25)	1·077 (2)
C(16)–H(16)	1·079 (2)	C(26)–H(26)	1·074 (2)
Fe(1)–N(11)–C(16)	123·9 (1)	Fe(1)–N(21)–C(26)	123·2 (1)
	124·3 (3)		123·3 (3)
Fe(1)–N(11)–C(12)	116·5 (1)	Fe(1)–N(21)–C(22)	116·8 (1)
	116·0 (3)		116·6 (3)
C(12)–N(11)–C(16)	119·3 (1)	C(22)–N(21)–C(26)	119·6 (1)
	119·4 (4)		119·7 (4)
C(13)–C(12)–N(11)	121·8 (1)	C(23)–C(22)–N(21)	121·5 (1)
	120·9 (5)		119·7 (5)
C(14)–C(13)–C(12)	118·8 (1)	C(24)–C(23)–C(22)	118·7 (1)
	119·4 (6)		120·1 (5)
C(15)–C(14)–C(13)	118·8 (1)	C(25)–C(24)–C(23)	119·3 (1)
	120·0 (6)		119·8 (6)
C(16)–C(15)–C(14)	119·3 (1)	C(26)–C(25)–C(24)	119·3 (1)
	118·8 (6)		118·4 (5)
N(11)–C(16)–C(15)	121·9 (1)	N(21)–C(26)–C(25)	121·6 (1)
	121·6 (5)		122·2 (5)
N(11)–C(12)–C(22)	114·9 (1)	N(21)–C(22)–C(12)	115·3 (1)
	115·4 (4)		115·6 (4)
C(13)–C(12)–C(22)	123·2 (1)	C(23)–C(22)–C(12)	123·1 (1)
	123·8 (5)		124·6 (5)
H(13)–C(13)–C(12)	121·5 (2)	H(23)–C(23)–C(22)	121·2 (2)
H(13)–C(13)–C(14)	119·7 (2)	H(23)–C(23)–C(24)	120·0 (2)
H(14)–C(14)–C(13)	119·5 (2)	H(24)–C(24)–C(23)	118·7 (2)
H(14)–C(14)–C(15)	121·7 (2)	H(24)–C(24)–C(25)	122·0 (2)
H(15)–C(15)–C(14)	121·8 (2)	H(25)–C(25)–C(24)	121·7 (2)
H(15)–C(15)–C(16)	118·9 (2)	H(25)–C(25)–C(26)	119·0 (2)
H(16)–C(16)–N(11)	116·9 (2)	H(26)–C(26)–N(21)	116·2 (2)
H(16)–C(16)–C(15)	121·2 (2)	H(26)–C(26)–C(25)	122·2 (2)

different from their average values of 1·389, 1·346 and 1·079 Å respectively. We can compare these lengths with the corresponding ones for pyridine [1·393 (1), 1·338 (1) and 1·083 (1) Å] obtained by microwave spectroscopy by Sorensen, Mahler & Rastrup-Andersen (1974). If we turn to the bond angles we find that the two pyridyl moieties, joined through C(21)–C(22), do not differ significantly, except at the Fe–N bond. This indicates that the unsymmetrical Fe–N bonding has little geometrical effect on the ligand. There are significant differences in the angles involving 'inner' and 'outer' half-pyridyl fragments. The mirror (σ_v) symmetry of pyridine has been distorted by up to 2° by the C(21)–C(22) bond and the ligation.

The ten C, N and D atoms in each pyridyl moiety are nearly coplanar as expected. The maximum distances from the respective least-squares planes are 0·014 Å for H(14) and 0·021 Å for H(25). The assumption of planarity gives $\chi = 5 \cdot 6$ and 6·7 for the two rings, showing small but significant non-planarity. The buckling shows no obvious pattern. The angle between the two rings is 7·4°. The rings are not coplanar with the Fe(1)N(11)N(21) plane, making angles of 10·0 and 11·5° with it.

The intramolecular bond lengths and angles for the hydrogenous compound at 4·2 K (*A*) and the deuterated at 115 K (*D*), given the slightly lower precision, do not differ significantly from the results above. The C–C and Fe–Cl (in $FeCl_4^-$) average bond lengths at 115 K are slightly shorter than at 4·2 K (1·388, 2·198 Å) but the difference is not enough to be able to say the 295 K X-ray apparent bond shortening is of thermal or valence origin. The angular distortions in the bipyridyl ligand at both 115 K and, for the hydrogenous compound, at 4·2 K show the same symmetry of pyridyl moieties and lack of mirror symmetry within the pyridyl fragment.

Intermolecular geometry

The intermolecular geometry is, not unexpectedly, complex. As expected there are no short intermolecular distances involving Fe atoms. There are also rather few short intermolecular distances which do *not* involve Cl atoms. These Cl contacts, which seem to determine the molecular packing of *both* $[FeCl_4]^-$ and $[Fe(bpy)_2Cl_2]^+$, are mainly Cl···C contacts (down to 3·30 Å) and Cl···H contacts (down to 2·65 Å). There are four independent Cl···C contacts less than 3·6 Å and six Cl···H less than 3·0 Å. In addition, there is a Cl(11)···Cl(21) contact of 3·90 Å. This latter might be expected to provide a weak but significant magnetic-exchange between Fe(1) and Fe(2). However, this pathway only provides one-dimensional chains. To produce three-dimensional magnetic exchange would involve long pathways through the bipyridyl ligands. This lack of effective, three-dimensional, magnetic-exchange pathways explains the low magnetic-ordering temperature of <4·2 K (Figgis *et al.*, unpublished).

Thermal motion

At 4·2 K we may expect only zero-point motion to be significant. The intramolecular modes become more significant at such low temperatures. We can expect values of $\langle U^2 \rangle$ due to internal modes of 1–2 × 10^{-3} Å^2 for the C,N atoms, 12–16 × 10^{-3} Å^2 for the H, 8–12 × 10^{-3} Å^2 for the D. We note the large zero-point motion associated with the H/D atoms (Willis & Pryor, 1975).

For the deuterated material at 4·2 K ($B+C$) we observe average mean-square displacements, $\bar{U}_{11}$, of 6 × 10^{-3} Å^2 for the Fe and Cl, 8 × 10^{-3} Å^2 for C and N, and 19 × 10^{-3} Å^2 for the D atoms. The corresponding figures for $\bar{U}_{33}$ are 8, 9 and 21 × 10^{-3} Å^2. As expected the D motion is about 10 × 10^{-3} Å^2 larger than that of the non-deuterium atoms. due to the C—D bends and stretches. The internal-mode contributions to non-hydrogen-atom motion appears to be small.

At 115 K the thermal motion is substantially increased – $\bar{U}_{11}$ is 21 × 10^{-3} Å^2 for Fe and Cl, 22 × 10^{-3} Å^2 for C and N, 40 × 10^{-3} Å^2 for D. For the 17 non-hydrogen atoms the increase in $\bar{U}_{11}$ is an almost uniform factor of 3·0 (5) (n = 17), while it is 2·1 (3) (n = 8) for the D atoms. The lower increase for D is ascribable to the internal modes, whose temperature dependence is very small. Examination of $\bar{U}_{33}$ gives similar figures of 2·9 (5) (n = 17) and 2·0 (7) (n = 8) respectively. If we subtract from D the expected intramolecular contribution of ~ 10 × 10^{-3} Å^2 from both the 4·2 and 115 K data we again obtain a ratio of ~3 for the increase in thermal motion. Such an increase corresponds, approximately, to a Debye temperature of about 80 cm^{-1} (or 115 K), a quite reasonable value for a partly molecular, soft, inorganic crystal.

The results for the hydrogenous compound at 4·2 K, when compared to the deuterated material, show an increase in $\bar{U}_{11}$ of 2·9 × 10^{-3} Å^2 in Fe and Cl motion, 2·4 × 10^{-3} Å^2 in C and N motion and 7·3 × 10^{-3} Å^2 in D/H motion. For $\bar{U}_{33}$ the corresponding figures are 4·2, 4·3 and 7·8 × 10^{-3} Å^2. An increase of 4 × 10^{-3} Å^2 is expected in zero-point motion from internal modes on substitution of H for D. The slight increase in motion of all atoms on hydrogenation is not expected or yet explained. The reason may be experimental (use of a small, perhaps biased, data set) or real (the force field in D and H materials may actually be different). The thermal motion at 295 K, derived from the X-ray data (Figgis, Patrick *et al.*, 1983), shows a further increase of approximately three in size over those at 115 K – showing the expected linearity in temperature.

The regular behaviour of the thermal parameters shows that the deuterated material is not markedly anharmonic. The satisfactory refinement allows us to conclude that this crystal is sufficiently well behaved as to be entirely suitable for spin and charge density studies.

We thank the Institut Laue–Langevin for access to the D15 diffractometer, and the Australian Research Grants Committee for financial support.

References

CHANDLER, G. S., FIGGIS, B. N., PHILLIPS, R. A., REYNOLDS, P. A., MASON, R. & WILLIAMS, G. A. (1982). *Proc. R. Soc. London Ser. A*, **384**, 31–48

FIGGIS, B. N., PATRICK, J. M., REYNOLDS, P. A., SKELTON, B. W., WHITE, A. H. & HEALY, P. C. (1983). Unpublished data.

FIGGIS, B. N., REYNOLDS, P. A. & MASON, R. (1982). *Proc. R. Soc. London Ser. A*, **384**, 49–55.

FIGGIS, B. N., REYNOLDS, P. A. & MASON, R. (1983). *J. Am. Chem. Soc.* **105**, 440–443.

FIGGIS, B. N., WILLIAMS, G. A., FORSYTH, J. B. & MASON, R. (1981). *J. Chem. Soc. Dalton Trans.* pp. 1837–1845.

KOESTER, L. (1977). *Springer Tracts Mod. Phys.* **80**, 36–39.

LEHMANN, M. S. & WILSON, S. (1979). Institut Laue–Langevin, Internal Report.

LE PAGE, Y. & GABE, E. J. (1979). *Acta Cryst.* A**35**, 73–78.

SORENSEN, G. O., MAHLER, L. & RASTRUP-ANDERSEN, N. (1974). *J. Mol. Struct.* **20**, 119–126.

STEWART, J. M., MACHIN, P. A., DICKINSON, C. W., AMMON, H. L., HECK, H. & FLACK, H. (1976). The XRAY76 system. Tech. Rep. TR-446. Computer Science Center, Univ. of Maryland, College Park, Maryland.

WILLIS, B. T. M. & PRYOR, A. W. (1975). *Thermal Vibrations in Crystallography*, pp. 191–196. Cambridge Univ. Press.